NIH Public Access
Author Manuscript
Biochemistry. Author manuscript; available in PMC 2009 November 25.

Published in final edited form as:
Biochemistry. 2008 November 25; 47(47): 12644–12654. doi:10.1021/bi8015857.

Biophysical Properties of Apolipoprotein E4 Variants: Implications in Molecular Mechanisms of Correction of Hypertriglyceridemia[χ]

Irina N. Gorshkova[‡,§,*], **Kyriakos E. Kypreos**[§,¶], **Donald L. Gantz**[‡], **Vassilis I. Zannis**[§], and **David Atkinson**[‡]

[‡]Department of Physiology and Biophysics, Boston University School of Medicine, 700 Albany Street, Boston, Massachusetts 02118

[§]Molecular Genetics, Whitaker Cardiovascular Institute, Departments of Medicine and Biochemistry, Boston University School of Medicine, 700 Albany Street, Boston, Massachusetts 02118

Abstract

In humans and animal models, high plasma concentrations of apolipoprotein (apo) E are associated with hypertriglyceridemia. It has been shown that overexpression of human wild-type (WT) apoE4 in apoE-deficient mice induces hypertriglyceridemia. In contrast, overexpression of an apoE4 variant, apoE4-mut1 (apoE4(L261A, W264A, F265A, L268A, V269A)), does not induce hypertriglyceridemia and corrects hypercholesterolemia. Furthermore, overexpression of another variant, apoE4-mut2 (apoE4(W276A, L279A, V280A, V283A)), induces mild hypertriglyceridemia and does not correct hypercholesterolemia. To better understand how these mutations improve the function of apoE4, we investigated the conformation and stability of apoE4-mut1 and apoE4-mut2 and their binding to dimyristoyl phosphatidylcholine (DMPC) vesicles and to triglyceride (TG)-rich emulsion particles. We found that the mutations introduced in apoE4-mut1 lead to a more stable and compactly folded conformation of apoE4. These structural changes are associated with a slower rate of solubilization of DMPC vesicles by apoE4-mut1 and reduced binding of the protein to emulsion particles as compared to WT apoE4. Under conditions of apoE4 overexpression, the reduced binding of apoE4-mut1 to TG-rich lipoprotein particles may facilitate the lipolysis of these particles and may alter the conformation of the lipoprotein-bound apoE in a way that favors the efficient clearance of the lipoprotein remnants. Mutations introduced in apoE4-mut2 result in smaller structural alterations compared to those observed in apoE4-mut1. The slightly altered structural properties of apoE4-mut2 are associated with slightly reduced binding of this protein to TG-rich lipoprotein particles and milder hypertriglyceridemia as compared to WT apoE4.

Human apolipoprotein E (apoE) is a key component of the lipoprotein transport system and is required for the maintenance of lipid homeostasis in the circulation and the brain (1–3). In humans, there are three natural apoE isoforms that differ from each other by amino acid substitutions at positions 112 and 158. ApoE3 (Cys-112, Arg-158) is the most common isoform; apoE2 (Cys-112, Cys-158) is associated with type III hyperlipoproteinemia, while apoE4 (Arg-112, Arg-158) is associated with high plasma cholesterol level and an increased risk for both coronary heart disease and Alzheimer's diseases (4–7). ApoE is one of the major protein constituents of triglyceride (TG)-rich chylomicrons and very low density lipoproteins

[χ]This work was supported by grants POHL 26335 and RO1 HL68216 from the National Institute of Heath

[*]To whom correspondence should be addressed: Department of Physiology and Biophysics, W-322, Boston University School of Medicine, 700 Albany Street, Boston, MA 02118. Fax: (617)638-4041. Phone: (617) 638-4207, igorshko@bu.edu.
[¶]Present address: Department of Medicine, University of Patras Medical School, Panepistimioupolis, Rio, TK 26500 Greece

NIH-PA Author Manuscript
NIH-PA Author Manuscript
NIH-PA Author Manuscript

NIH-PA Author Manuscript

NIH-PA Author Manuscript

NIH-PA Author Manuscript

(VLDL). In the bloodstream, these TGrich lipoproteins are converted into remnants through hydrolysis of their core TG by lipoprotein lipase (LPL). At physiological concentrations, apoE mediates the hepatic uptake of the lipoprotein remnants via the low density lipoprotein (LDL) receptor and thereby, regulates plasma lipid levels and contributes to atheroprotection (1–3, 7). However, elevated plasma apoE levels in humans and in animal models have been positively correlated with hypertriglyceridemia (8–10). It has been shown that overexpression of wild-type (WT) apoE in apoE-deficient ($apoE^{-/-}$) mice triggers hypertriglyceridemia due to increased VLDL TG secretion and impaired VLDL lipolysis (9–10).

Induction of hypertriglyceridemia in mice overexpressing apoE was prevented by Cterminal truncations of apoE, suggesting that the 260–299 region of apoE is essential for induction of hypertriglyceridemia (10,11). In an attempt to further identify specific residues and regions of the C-terminal segment of apoE involved in the induction of hypertriglyceridemia, two apoE4 variants, apoE4-mut1 (apoE4(L261A, W264A, F265A, L268A, V269A)) and apoE4-mut2 (apoE4(W276A, L279A, V280A, V283A)) (Figure 1), were generated and studied in *vivo* in $apoE^{-/-}$ mice using adenovirus-mediated gene transfer (17). Each of these variants has alanine substitutions for hydrophobic residues in one of two hydrophobic stretches of amino acids, 261–269 or 276–283, that are thought to be involved in lipid and lipoprotein binding of apoE (16,18–20). These studies showed that overexpression of apoE4-mut1 in $apoE^{-/-}$ mice corrected hypercholesterolemia and did not induce hypertriglyceridemia. In contrast, comparable levels of expression of apoE4-mut2 did not correct hypercholesterolemia and induced mild hypertriglyceridemia (Figure 1, inset). The molecular basis for the improved function of these apoE4 variants is not fully understood. The results of the animal studies suggested that mutations introduced in apoE4-mut1, and to a lesser extent in apoE4-mut2, may decrease the ability of apoE4 to be associated with TG-rich lipoproteins in plasma (17). The decreased affinity of the apoE4 variants to TG-rich particles could explain, in part, the improved function of these variants. However, no direct experimental evidences of the altered ability of apoE4-mut1 and apoE4-mut2 to bind to TG-rich particles have been obtained.

Here, we studid *in-vitro* the ability of apoE4-mut1and apoE4-mut2 to bind to synthetic VLDL-like particles and to solubilize dimyristoylphosphatidylcholine (DMPC) vesicles. VLDL-like emulsion particles prepared from triolein and phosphatidylcholine (PC) were utilized as a model for TG-rich lipoproteins (21,22). To better understand how the mutations introduced in apoE4-mut1and apoE4-mut2 alter the function of apoE4, we investigated the conformation and stability of the apoE4 variants. Previous studies have shown that the structural and biophysical properties of apoE dictate the function of the protein (15,16,19). For example, apoE4 has increased domain interaction and more loose tertiary structure, as compared to apoE2 and apoE3, which is thought to lead to the preferential binding of apoE4 to large VLDL and the preferential binding of apoE3 and apoE2 to smaller high density lipoprotein in plasma (23,24). The conformational stability of the common isoforms of apoE correlates inversely with the rate of their association with phospholipid vesicles and the affinity of the isoforms to TG-rich emulsion particles (25–27). We found that the E4-mutlvariant that prevents the induction of hypertriglyceridemia has a more compactly folded and stable structure and a reduced ability to solubilize DMPC vesicles and to bind to TG-rich particles as compared to WT apoE4. In contrast, the E4-mut2 variant that induces milder hypertriglyceridemia, compared to WT apoE4, has milder changes in the conformation and stability and the ability to solubilize DMPC vesicles and to bind to TG-rich particles.

EXPERIMENTAL PROCEDURES

Materials

Materials not mentioned in the Experimental procedures have been obtained from sources described previously (17,28,29).

NIH-PA Author Manuscript

NIH-PA Author Manuscript

NIH-PA Author Manuscript

Construction of Recombinant Adenoviruses, Expression, Purification and Preparation of Proteins—The generation of recombinant adenoviruses carrying the genomic sequence for the WT, apoE4-mut1 (apoE4(L261A, W264A, F265A, L268A, V269A)), and apoE4-mut2 (apoE4(W276A, L279A, V280A, V283A)) has been described previously (17). For apoE4 production, human HTB13 cells in roller bottles were infected with adenoviruses expressing the WT or the mutant apoE4 forms and the medium was harvested as described previously (30). Purification of apoE from the culture medium was performed using dextran sulfate-Sepharose column as described before (30). The purified proteins were analyzed by 12% SDS-PAGE and by Western blotting. Fractions containing apoE4 of >95% purity were dialyzed against 5 mM ammonium bicarbonate, lyophilized, and stored at −80°C. Before use in the experiments, lyophilized proteins were dissolved in a solution containing 6 M guanidine hydrochloride (GdnHCl) and 1% (v/v) β-mercaptoethanol and dialyzed extensively against an appropriate buffer.

Circular Dichroism (CD) Spectroscopy—CD-measurements were performed on an AVIV 62DS or AVIV 215 spectropolarimeter (AVIV Associates, Inc.) equipped with a thermoelectric temperature control and calibrated with d-10-camforsulfonic acid in 2, 5, and 10 mm path length quartz cuvettes as previously described (29,31). Proteins were in 10 mM sodium phosphate buffer (pH 7.4), freshly dialyzed from 6 M GndHCl and 1% β-mercaptoethanol solution. Far-UV CD spectra were recorded from 260 to 185 nm at 25°C; for each sample, three to five scans were performed and averaged. The thermally induced unfolding of the proteins was monitored by ellipticity at 222 nm over the temperature range 5 to 90°C at two heating rates, 0.25°C/min and 0.65°C/min. Because of the high tendency of full size apoE to aggregate (32), the experiments were performed at relatively low protein concentrations, 10–30 μg/mL, including the lowest possible concentration for each particular experiment. For each apoE4 form, spectra and melting curves were recorded at several protein concentrations within the indicated range and then, after the baseline subtraction, were normalized to molar residue ellipticity [Θ]. The α-helix content was estimated from the molar residue ellipticity at 222 nm, $[\Theta_{222}]$ (33).

For analysis of thermal unfolding, the fraction of unfolded protein at a given temperature was determined from the equation:

$$\text{Unfolded Fraction}=([\Theta_{222}]_F - [\Theta_{222}])/([\Theta_{222}]_F - [\Theta_{222}]_U),$$

where $[\Theta_{222}]$ is a molar residue ellipticity at a given temperature and $[\Theta_{222}]_F$ and $[\Theta_{222}]_U$ are molar residue ellipticity for the protein in folded (native) and unfolded (thermally denaturated) states, respectively. The values for the unfolded fraction were plotted against temperature and the data were smoothed over a five degree window. The data $[\Theta_{222}]$ were algebraically differentiated with respect to temperature and the derivative function $d[(\Theta_{222})]/dT$ was plotted against temperature. For each thermal unfolding curve, the apparent melting temperature was determined as the midpoint of thermal unfolding at which unfolding of apoE was half complete, $T_{1/2}$, and as the maximum of the first derivative function, T^d_m (34). The width of the first derivative function $d[\Theta_{222}]/dT$ at the half maximal height, $\Delta(d[\Theta_{222}]/dT)$, was determined for each protein to compare cooperativity of unfolding of the proteins (34).

ANS (8-Anilino-2-naphthalene-sulfonate) Fluorescence Measurements—ANS fluorescence emission spectra were collected on a FluoroMax-2 fluorescence spectrometer (Instruments S.A., Inc.) as previously described (28,29). Fluorescence of ANS was recorded in Tris buffer (10 mM Tris-HCl, 150mM NaCl, 0.02% NaN3, 1 mM EDTA, pH.7.4) at ANS concentration 125 μM in the presence of 25 μg/ml (0.74 μM) apoE4 or in the absence of any protein. To control possible effects of apoE4 aggregation, the experiments were repeated at

NIH-PA Author Manuscript

NIH-PA Author Manuscript

NIH-PA Author Manuscript

ANS concentration 250 μM in the presence of 50 μg/ml (1.48 μM) apoE4. This increase in apoE4 concentration had no effect on the results of the experiment that is consistent with the absence of the protein self-association at the indicated concentrations. In each experiment, ANS fluorescence was also recorded in the presence of the "reference" proteins, carbonic anhydrase or bovine serum albumin, at the corresponding concentrations. Wavelength of maximum fluorescence (WMF) and intensity of fluorescence emission at WMF were determined from each spectrum.

DMPC Turbidity Clearance Studies—The solubilization of DMPC multilammelar vesicles by apoE was studied according to modified procedures (25,35,36). To prepare the vesicles, 1 mg of DMPC was dissolved in 1 ml of 2:1 (v/v) chloroform/ methanol solution, dried under nitrogen to form a thin lipid film, and left overnight under vacuum to get rid of any traces of the organic solvent. The lipids were then resuspended in 1 ml of Tris buffer containing 0.1M GndHCl and vortexed vigorously for 1–2 min to become milky turbid suspension. The 0.1 M GndHCl was added to the buffer to ensure the absence of apoE self-association during the experiment; this low denaturant concentration has been shown to have no effect on the protein conformation and the turbidity clearance data (25). For the clearance experiments, ~ 0.95 ml of the stock suspension diluted to the lipid concentration 60 μg/ml was placed in 1 cm path length quartz cuvett and preincubated for 5 min at 24°C within a holder of a spectrophotometer (Varian Cary-300) with thermoelectric temperature control. Monitoring of absorbance at 325 nm indicated no significant changes in turbidity of the lipid suspension during the preincubation. A small volume of apoE in Tris buffer (freshly dialyzed from 6 M GdnHCl and 1% (v/v) β-mercaptoethanol) was added to the lipid suspension in the cuvette to give a protein concentration of 7.5 μg/ml (0.22 μM) and gently mixed by repeated pipetting within 10 s before resuming the recording of absorbance at 325 nm. In the control experiments, buffer containing no protein was added to the cuvette with the lipid suspension. After recording turbidity for 2 to 4 hrs, the apoE/DMPC mixtures were left overnight in the cuvettes within the spectrophotometer holders maintaining the controlled temperature of 24°C to be observed under electron microscope the following morning, after 20 h of incubation.

Preparation of TG-rich Emulsion Particles—TG-rich emulsion particles were prepared by sonication followed by ultracentrifugation according to modified procedures (22,37) originally developed by Miller and Small (21). Chloroform solutions of 100 mg triolein and 25 mg egg yolk PC were mixed together, dried under nitrogen and vacuum desiccated overnight at 4 °C. The dried lipids were suspended in 20 ml of Tris buffer and sonicated at 80–90 watts continuous power using a Branson sonifier, model 350, with a flat tip. Sonication was performed for 20 min under a stream of nitrogen; the temperature of the sample was maintained at 40–50°C by immersion in an ice-water bath. The sonicated mixture was transferred into centrifuge tubes, overlayered with warm Tris buffer and centrifuged in an SW41 rotor (Beckman, CA) at 20°C for 15 min at 18,000 rpm. A top creamy layer and an under-laying cloudy layer containing large chylomicronlike particles were removed by tube slicing. The remaining sample was transferred into a new tube, overlayered with Tris buffer and centrifuged in the same rotor at 20°C for 1 h at 25,000 rpm. The top layer was recovered as TG-rich emulsion and analyzed by phospholipids and triglyceride assays to determine composition and by electron microscopy to examine morphology and determine particle size. The emulsions were used for the binding assays within 2 days after isolation; during this period no changes were detected on the electron microscopy photographs.

Binding of ApoE4 to Emulsion Particles—Binding of apoE4 to emulsion was studied according to modified procedures (22,37). To minimize the required amounts of nonlabeled apoE4 forms, a fixed amount of the proteins was incubated with various amounts of emulsion. Specifically, 80 μg of WT apoE4, apoE4-mut1, or apoE4-mut2 (freshly dialyzed from 6 M

NIH-PA Author Manuscript

NIH-PA Author Manuscript

NIH-PA Author Manuscript

GdnCHl and 1% β-mercaptoethanol) were incubated with increasing amounts of emulsion in 1.4 ml of Tris buffer to give a PC to protein molar ratio ranging from 50 to 1020. Incubation was performed for 1 h at 27°C in a water bath with gentle shaking. Then each mixture was overlayered with NaCl solution of the density 1.006 g/cm^3 and spun in an SW60 rotor for 80 min at 40,000 rpm at 25 °C. The emulsions floating to the top of the tubes were recovered by tube slicing; they contained emulsionbound apoE4. Lipid-free apoE4 was in the bottom fractions. The concentration of bound apoE was calculated by subtracting the background free apoE concentration in the top fractions as described (37). Emulsions from four different preparations were used for the binding assays. With each isolated emulsion, four to six emulsion/apoE4 mixtures with various PC to protein ratios were studied for each protein.

Electron Microscopy—Analysis of the morphology and estimation of the size of isolated TG-rich emulsion particles and apoE/DMPC complexes were performed using negative staining electron microscopy as described (36). Emulsions were appropriately diluted; apoE/DMPC complexes were processed without dilution. Images of random fields of particles were recorded on Kodak SO-163 film (Eastman Kodak Co, Rochester, NY) using a CM12 electron microscope (Philips Electron Optics, Eindhoven, The Netherlands).

Analytical Procedures—Protein concentrations were determined by the Lowry procedure (38) and by absorbance at 280 nm with the extinction coefficient 1.34 ml/ (mg cm). TG concentration was determined by Infinity™ TG Kit (Thermo Electron, Australia). PC concentration was determined by Bartlett phosphorus assay (39).

RESULTS

CD Analysis of the α-Helical Content and Thermal Unfolding

Far-UV CD data were recorded at protein concentrations 10–30 μg/mL in 10 mM sodium phosphate buffer, pH 7.4. Because of the high tendency of apoE to aggregate, spectra and thermal unfolding for each apoE4 form were recorded at several protein concentrations within the indicated range. No changes in the normalized spectra or normalized melting curves were observed with the variations in the protein concentration, which is consistent with the absence of protein self-association within the range of the concentrations used in our experiments. This agrees with previous data (40,41) showing that apoE4 is largely monomeric at the low concentrations used in the CD studies. The α-helical content of the apoE4 forms (Table 1) was estimated from the normalized far-UV spectra. The α-helical content of WT apoE4 was ~62% that corresponds to ~189 residues in the helical conformation. The value for the α-helical content of WT apoE4 is within the range of the previously published estimations, 46 to 64% (16,42,43). There was no significant difference between the α-helical content of apoE4-mut2 and WT apoE4, although in all the experiments, apoE4-mut2 consistently exhibited slightly lower values for α-helicity. In contrast, apoE4-mut1 had ~11% lower α-helical content compared to WT apoE4 that corresponds to ~34 fewer residues in the helical conformation of this variant.

To investigate stability of the apoE4 forms, thermally induced unfolding of the proteins was monitored using CD. The thermal unfolding curves plotted as a fraction of unfolded protein against temperature are shown in Figure 2A. The values of the midpoint of thermal unfolding at which the protein is half unfolded, $T_{1/2}$, are shown in Table 1. The shifts of the unfolding curves for the mutants to higher temperatures suggest a trend in stability (WT apoE4 < apoE4-mut2 < apoE4-mut1), consistent with the changes in $T_{1/2}$ in the same order. However, the differences in $T_{1/2}$ between apoE4-mut2 and the other proteins are not statistically significant. Figure 2B shows the first derivative functions $d[\Theta_{222}]/dT$ of the thermal unfolding curves that emphasize differences in slope for the unfolding curves. Parts of the derivative function at low

NIH-PA Author Manuscript

NIH-PA Author Manuscript

NIH-PA Author Manuscript

and high temperatures that correspond to less cooperative structural changes in each protein are not shown because of the high proportion of noise in these parts of the derivative function. The temperature of the maximum of the derivatives curves, T^d_m, are in agreement with the midpoint of thermal unfolding $T_{1/2}$ (Table 1), which is consistent with reversibility of the thermal unfolding of the proteins. Similar to the values for $T_{1/2}$, the values for the apparent melting temperature T^d_m indicate an increase in the stability of the apoE4 variants compared to WT apoE4.

The width of the first derivative function $d[\Theta_{222}]/dT$ at the half maximal height, $\Delta(d[\Theta_{222}]/dT)$, which is inversely proportional to the apparent van't Hoff enthalpy of the transition (34), decreases in the order WT apoE4 > apoE4-mut2 ≥ apoE4-mut1 (Table 1). This is consistent with the higher cooperativity of unfolding of the variant proteins, especially apoE4-mut1, compared to WT apoE4, in the temperature region ~27 to ~70°C. The heights of the peaks for the derivative functions $d[\Theta_{222}]/dT$, which is greatest for apoE4-mut1, slightly lower for apoE4-mut2, and significantly lower for apoE4 (Figure 2B), agrees with the trend in cooperativity of unfolding: WT apoE4 < apoE4-mut2 ≤ apoE4-mut1.

ANS Binding

To explore changes in the tertiary structure of the variant apoE4 forms, we monitored intrinsic fluorescence of the amphipathic fluorescent dye ANS in the presence of WT apoE4, apoE4-mut1, and apoE4-mut2 (Figure 3). The intrinsic fluorescence of ANS is known to be increased and red-shifted when the dye is bound to protein hydrophobic surfaces or cavities, while the water-phase dye does not contribute to the emission. Table 2 shows parameters of ANS fluorescence in the presence of the apoE4 forms and the "reference" proteins, carbonic anhydrase as a typical globular watersoluble protein and bovine serum albumin as a protein exposing hydrophobic binding pockets (data for bovine serum albumin not shown in Figure 3). Of all three apoE4 forms, WT apoE4 results in the largest intensity and red shift of ANS fluorescence suggesting a loosely folded conformation with the greatest exposure of hydrophobic surfaces. For apoE4-mut2, compared to WT apoE4, there is a ~10% decrease in the intensity and a ~6 nm red shift of ANS fluorescence, that suggests a reduction of exposed hydrophobic surfaces and a more compact folding of apoE4-mut2. In the presence of apoE4-mut1, the ANS fluorescence spectrum changes most dramatically compared to the fluorescence in the presence of WT apoE4: 50% decrease in the intensity and ~9 nm red shift that indicates a significant reduction in exposed hydrophobic sites. The data suggest that of the three apoE4 forms, apoE4-mut1 has a most compactly folded structure and WT apoE4 has a most loosely folded structure.

DMPC Turbidity Clearance

Electron microscopy of apoE4/DMPC mixtures. To analyze the kinetics of solubilization of lipid vesicles by the apoE4 forms, we used a standard apolipoprotein DMPC-binding assay that examines the clearance of DMPC multilamellar vesicles by the apolipoproteins. The clearance of DMPC vesicles was triggered by adding a protein and monitored by turbidity at 325 nm. In order to avoid oligomerization of the full-size apoE forms, the clearance experiments were performed at a very low protein concentration (7.5 μg/ml). This resulted in a lower apolipoprotein:lipid weight ratio (1:8) in our experiments compared to the ratio 1:2.5 or 1:2 in similar experiments described elsewhere (25,36).

The time-courses for clearance of DMPC vesicles by apoE4 forms (Figure 4) show that the mutations introduced in apoE4-mut2 do not affect significantly the rate of solubilization of the lipid vesicles by E4. In contrast, apoE4-mut1 clears the turbidity significantly slower than WT apoE4 and apoE4-mut2 indicating a lower rate of solubilization of DMPC vesicles by apoE4-mut1. Residual turbidity was significantly higher for apoE4-mut1 than for WT apoE4

NIH-PA Author Manuscript

NIH-PA Author Manuscript

NIH-PA Author Manuscript

suggesting the presence of larger particles in the apoE4-mut1/DMPC mixture. To confirm this, we performed electron microscopy analysis of the mixtures WT apoE4/DMPC and apoE4-mut1/DMPC after 20 h preincubation at 24°C. The micrographs show the presence of discoidal particles in both mixtures (Figure 5). The discoidal particles are apoE4:DMPC complexes formed during the incubation; they are seen "face-up" or stacked on edge in short rouleaux produced during the negative staining process. The average thickness of the discoidal particles measured from the periodicity of discs stacked in rouleaux is (5.7±0.5) nm that is consistent with the thickness of DMPC bilayer discs determined previously (44). The estimated average diameter of the discoidal particles was similar (~20.5 ± 2.5 nm) for particles formed by WT apoE4 and by apoE4-mut1. However, the apoE4-mut1/DMPC mixtures (Figure 5B) contain fewer discoidal complexes and shorter rouleaux than the WT apoE4/DMPC mixtures (Figure 5A) indicating significantly lower production of the discoidal protein-lipid particles by apoE4-mut1. Furthermore, the micrographs of the apoE4-mut1/DMPC mixtures show the presence of large lipid vesicles that are the remaining DMPC vesicles not solubilized by the proteins, consistent with the lower lipidbinding ability of apoE4-mut1.

Binding of apoE4 Forms to Emulsion Particles

Emulsion particles were made from triolein and egg yolk PC and used as a model for TG-rich lipoproteins. The triolein to PC weight ratio in the emulsions was 3.9 ± 0.3 (mean ± SD of six isolated emulsion). Thus, triolein was the major component of emulsion particles accounting for almost 80% of the total mass. The average size of particles in a typical isolated emulsion calculated from the electron micrographs was 55 ± 25 nm (mean ±SD, n=198). The large standard deviations reflect a broad size distribution that resembles a size distribution of plasma VLDL. Importantly, variations in the particle composition and size between different isolated emulsions used in our studies were insignificant.

To investigate if the mutations made in apoE4-mut1 and apoE4-mut2 affect the ability of apoE4 to bind to TG-rich emulsion particles, WT apoE4 and each of the variants were incubated with emulsions at various PC to protein molar ratios ranging from 50 to 1020. The emulsion-bound protein and unbound protein were then separated by ultracentrifugation of the mixtures. For each apoE4 form, a portion of the emulsionbound protein was plotted versus a PC to protein molar ratio in the incubation mixtures (Figure 6). This presentation of results of the binding assays was chosen over plotting a concentration of the emulsion-bound protein versus a concentration of the unbound protein (24,37), as our binding assays were performed using the fixed amount of protein and the increasing amounts of emulsion. The plots in Figure 6 indicate that at each PC/protein ratio, the portion of the bound protein is the highest for WT apoE4, slightly lower for apoE4-mut2, and significantly lower for apoE4-mut1. The plots in Figure 6 represent results of binding assays performed with one of four isolated emulsions. Similar results were obtained in binding assays performed with each other isolated emulsion. However, because binding assays performed with emulsions from different preparations might be carried out at slightly different PC/protein ratios, the standard deviations for the portion of bound protein in Figure 6 are shown only for the PC/protein molar ratio of 255 and 600, as three to five binding assays for each protein were performed at the PC/protein ratio of 255 ± 5 and 600 ± 7 (mean ± SD). At these both values of the PC/protein ratio, the average portion of the bound protein decreases in the order: WT apoE4 ≥ apoE4-mut2 > apoE4-mut1 (Table 3).

To analyze the relative content of apoE4 on the resultant apoE4-emulsion complexes formed during the incubation, the bound protein to PC weight ratio was determined in the top fractions recovered after ultracentrifugation following incubation. The values for this ratio in terms of a number of amino acids of bound protein per molecule of PC for the incubations with the initial PC/protein molar ratio of 255 ± 5 and 600 ± 7 are listed in Table 3. Regardless of the initial proportion between apoE4 and emulsion during the incubation, the number of amino

NIH-PA Author Manuscript

NIH-PA Author Manuscript

NIH-PA Author Manuscript

acids per PC molecule in the protein-emulsion complexes is lower for apoE4-mut1 by almost 50% compared to WT apoE4 and by almost 40% compared to apoE4-mut2. Figure 7 shows the numbers of bound apoE4 molecules per emulsion particle at various initial PC to protein molar ratios in the incubation mixtures containing WT apoE4 or apoE4-mut1.The number of bound apoE4 molecules per emulsion particle was calculated from the molar ratio of the bound protein to PC in the top fractions recovered after ultracentrifugation, the average emulsion particle diameter, and the assumptions that the emulsion surface area per amino acid residue in a helix is 0.15 nm^2 (45,46) and the emulsion surface area covered by one PC molecule is 0.7 nm^2 (47). The data in Figure 7 show that at each initial PC to protein ratio, less apoE4-mut1 molecules, than WT apoE4 molecules, are bound to one emulsion particle. At each initial PC to protein ratio, there was a trend for the numbers of apoE4 molecules per particle: WT apoE4 ≥ apoE4-mut2 > apoE4-mut1 (data for apoE4-mut2 not shown in Figure 7).

DISCUSSION

It has been shown that $apoE^{-/-}$ mice overexpressing human WT apoE develop severe hypertriglyceridemia (9,10). Development of hypertriglyceridemia may be prevented by specific mutations of apoE (10,11,17). In this work, we studied the properties of two apoE4 variants, apoE4-mut1 (apoE4(L261A, W264A, F265A, L268A, V269A)) that leads to normal plasma triglyceride and cholesterol levels and apoE4-mut2 (apoE4(W276A, L279A, V280A, V283A)) that leads to mild hypertriglyceridemia and hypercholesterolemia when these variants are overexpressed in $apoE^{-/-}$ mice. We were trying to identify alterations in the structural, stability and lipid and lipoprotein-binding properties of these apoE4 variants to better understand how the mutations introduced in these apoE4 forms favorably change the protein function. Particularly, we investigated binding of the apoE4 variants to synthetic VLDL-like emulsion particles as a model of plasma large TG-rich lipoproteins and their remnants. It has been established that apoE bound to TG-rich lipoproteins and their remnants modulates the catabolism of plasma triglycerides (9,17,48,49).

According to the CD analysis, apoE4-mut1 has significantly fewer number of residues in the α-helical conformation than apoE4-mut2 and WT apoE4 (~155 vs. ~183 and ~189, correspondingly). This indicates that mutation of five hydrophobic and bulky residues in the 8-residue segment 261–269 in apoE4-mut1 results in a loss of ~34 residue in the helical conformation of apoE4. In contrast, mutation of four hydrophobic and bulky residues in the 8-residue segment 276–283 in apoE4-mut2 results in a smaller loss of helical residues (~6 residues). This suggests that residues within the segment 261–269 may be involved in tertiary (inter-helical) interactions. Disruption of these interactions by the amino acid substitutions in this segment results in unfolding of ~34-residue helical segment(s), including likely the 261–269 segment and ~ 26-residue segment(s) in other part(s) of the molecule, perhaps in the N-terminal domain. In the amino acid sequence of apoE4, residues 261–269 are close to Glu255 that forms a putative salt bridge with Arg61 that is thought to stabilize a close contact between the protein N- and C-terminal domains (19,50). Mutations made in apoE4-mut1 may change the protein conformation in the vicinity of Glu255 and thus obstruct the salt-bridge formation with Arg61. This may result in disruption of intra-molecular interactions involved in stabilizing the α-helical structure of those apoE4 segments (consisting of ~26-residues) that are unfolded in apoE4-mut1 and may be located in the N-terminal domain. In contrast, the mutated residues in apoE4-mut2 located within the segment 276–283 are more remote from Glu255 in the amino acid sequence. Therefore, mutations made in apoE4-mut2 have likely only a local effect on the protein conformation (a loss of ~6 helical residues in the mutated region) and a less significant effect on the salt bridge between Glu255 and Arg61 and domain interaction.

According to the ANS studies, mutation of the hydrophobic and bulky residues between amino acids 261 and 269 in apoE4-mut1 results in significantly fewer exposed hydrophobic surfaces

NIH-PA Author Manuscript

NIH-PA Author Manuscript

NIH-PA Author Manuscript

in apoE4. This agrees with the existence of a largely exposed hydrophobic site created by residues 261–272 in apoE4 (16,40). It appears that the compactness of the protein structure is increasing in the order: WT apoE4 ≤ apoE4-mut2 < apoE4-mut1, while the α-helical content is decreasing in the same order. These data suggest that the salt bridge between Glu255 and Arg61 in apoE4 may create spatial constraints that hinder compact tertiary folding of the protein. Eliminating (weakening) this salt bridge in apoE4-mut1 (and in a much lesser extent in apoE4-mut2) is associated with unfolding of some helical regions and eliminating (weakening) the spatial constraints that allows more compact protein folding.

Not withstanding the reduced helical secondary conformation, the more compact structure of apoE4-mut1 appears to be more stabilized and to unfold more cooperatively than a relatively loosely folded structure of WT apoE4 (Figure 2, Table 1). The increased stability of apoE4-mut1, in spite of the fewer number of residues in the helical conformation of the protein (Table 1), suggests that tertiary interactions stabilizing the compactly folded conformation of apoE4-mut1 are more resistant to heat than interactions stabilizing the conformation of WT apoE4, including domain interaction and interactions stabilizing the additional 34-residue helical segment(s). Interestingly, the conformational stability of apoE3 isoform is higher than stability of apoE4 isoform (41,42), also in spite of the absence of domain interaction (16) and a lower α-helical content in apoE3 (by ~5–10%, our data). Similarly, apoE3 is more compactly folded than apoE4 (24). More cooperative thermal unfolding of apoE4-mut1 suggests that this variant is less prone to form a stable folding intermediate than more loosely folded WT apoE4. This may have a beneficial effect on the function of apoE4-mut1-containing lipoproteins, because the increased propensity of apoE to form partially folded stable intermediates is thought to be implicated in abnormal lipoprotein metabolism (51,52).

The more stabilized conformation of apoE4-mut1 that is likely less prone to form stable intermediate is associated with a significant reduction in lipid binding, in agreement with the observed inverse correlation between stability and DMPC binding for full-size apoE (25,26, 52). ApoE4-mut1shows a significant reduction in both the rate and ability to associate with DMPC vesicles (Figure 4 and Figure 5) and the ability to bind to TG-rich emulsion particles (Figure 6). The reduced total length of α-helices in apoE4-mut1 (~34 helical residues less then in WT apoE4) may contribute to the reduced lipid-binding of this protein, because the total length of helices in an apolipoprotein determines its association with lipids (53). Fewer exposed hydrophobic sites and more compact tertiary conformation of apoE4-mut1 can also contribute to the slower rate and ability of this mutant to associate with phospholipid vesicles and the ability to bind to TG-rich particles.

The reduced ability of apoE4 to solubilize multilamellar phospholipid vesicles and bind to TG-rich lipoproteins may have a crucial effect on lipoprotein metabolism and plasma lipid levels. ApoE bound to TG-rich lipoproteins directly inhibits the LPL-mediated lipolysis of TG by promoting substrate dissociation from LPL (48). Thus, reduced binding of apoE to TG-rich particles will promote LPL-mediated hydrolysis of the particles. Also, studies of animal models overexpressing apoE suggested that hypertriglyceridemia developed in these animals results partially from displacement of apoC-II from TG-rich lipoproteins by apoE (9,54). Apo C-II is required for the activation of LPL (55); thus, the association of apoC-II with the TG-rich lipoproteins enhances the lipolysis of their TG. Mutations made in apoE4-mut1 result in the conformational and stability changes that reduce significantly the binding of apoE4 to TG-rich lipoproteins and thus favor the increased binding of apoC-II that promotes LPL-mediated lipolysis and clearance of lipoprotein remnants.

The conformational and stability characteristics and ability to bind to TG-rich particles for apoE4-mut2 appear to be between the characteristics for WT apoE4 and apoE4-mut1. The α-helical content, ANS fluorescence intensity that correlates with the exposure of hydrophobic

NIH-PA Author Manuscript

NIH-PA Author Manuscript

NIH-PA Author Manuscript

surfaces, the protein destabilization and the ability to bind to TG-rich model particles decrease in the order: WT apoE4 ≥ apoE4-mut2 > apoE4-mut1. The in vivo studies showed that under conditions of overexpression of apoE4-mut2, these slightly altered properties of the protein are associated with milder hypertriglyceridemia (Figure 1, inset).

The data in Figure 7 show that one emulsion particle binds less apoE4-mut1 molecules than WT apoE4-molecules throughout the entire range of the initial PC/protein ratios in the incubation mixtures (from 1025 to 40). The extrapolation of these data to the conditions of protein saturation (the initial ratio PC/protein ⟶ 0) suggests that under these conditions, when a maximal possible amount of protein is bound to emulsion, the emulsion surface will also accommodate fewer molecules of apoE4-mut1 than WT apoE4. This suggests that one molecule of WT apoE4 occupies a smaller area on emulsion particles than one molecule of apoE4-mut1. Compared to apoE4-mut1, WT apoE4 molecule may be more deeply immersed into the lipid layer or/and have more compact conformation on the emulsion surface. This may imply that under conditions of apoE overexpression, when the protein concentration in plasma and on TG-rich lipoproteins is high, the receptor binding region of WT apoE4 may be buried or masked and thereby unable to mediate clearance of the lipoproteins. It has been suggested that at high surface concentrations of apoE4 on TG-rich particles, the whole N-terminal domain of the protein may even be displaced from the lipid surface and adopt a “closed” fourhelix bundle conformation (37,56) that precludes the interaction of the receptor-binding region with the LDL-receptor and impairs clearance of remnant lipoproteins (57). In contrast, under conditions of overexpression of apoE4-mut1, each protein molecule occupies a larger area on the emulsion surface that may allow the “open” lipid-bound conformation of the N-terminal domain. In this conformation, the receptor-binding region of apoE is recognized by the LDL receptor and thus may promote the efficient clearance of the apoE-containing lipoproteins. This may also explain why, in contrast to WT apoE4, overexpression of apoE4-mut1 corrects hypercholesterolemia and does not induce hypertriglyceridemia. The amounts of apoE4-mut2 bound to emulsion are not significantly different from the corresponding amounts of WT apoE4 (Table 3). This may imply that under conditions of overexpression of apoE4-mut2, the topology and conformation on the emulsion surface for this variant are similar to those of WT apoE4, so that the receptor-binding region of apoE4-mut2 may be buried or masked, or the whole N-terminal domain of this mutant may be displaced from the particle surface. This may explain why overexpression of apoE4-mut2, similar to WT apoE4, is associated with hypercholesterolemia and hypertriglyceridemia.

It appears that the mutations made in apoE4-mut1 lead to changes in the biophysical characteristics of apoE4 that make it resemble apoE3. The interaction between the N- and C-terminal domains is a characteristic of apoE4 and does not exist in apoE3 (15,19). Our studies suggest that the domain interaction may be also reduced in apoE4-mut1 compared to WT apoE4. ApoE3, similar to apoE4-mut1, has a more compactly folded conformation as shown by ANS fluorescence (24), is more stable (41,42), solubilizes DMPC vesicles slowly (25,40), and has a reduced ability to bind to TG-rich emulsion particles as compared to WT apoE4 (24). This “conversion” of apoE4 into apoE3-like protein by the (L261A, W264A, F265A, L268A, V269A) mutation is associated with normalization of plasma lipid levels of $apoE^{-/-}$ mice without induction of hypertriglyceridemia. It has been established that in humans, the most common isoform apoE3, in contrast to apoE4, is not associated with high plasma cholesterol level and an increased risk of development of atherosclerosis (1–3,7). However, similar to apoE4, apoE3 at high plasma concentrations is associated with hypertriglyceridemia (8–11). In contrast, overexpression of apoE4-mut1 in $apoE^{-/-}$ mice does not induce hypertriglyceridemia. The bigger differences in some properties between WT apoE4 and apoE4-mut1, compared to the differences in these properties between WT apoE4 and apoE3, may be a key to the beneficial effects of the mutations made in apoE4-mut1. For example, both apoE3 and apoE4-mut1 have less exposed hydrophobic surfaces than WT apoE4 as shown by

NIH-PA Author Manuscript

NIH-PA Author Manuscript

NIH-PA Author Manuscript

ANS fluorescence data; however, ANS intensity in the presence of WT apoE4 is only ~1.2 times larger than the intensity in the presence of apoE3 (58) but two times larger than in the presence of apoE4-mut1 (Table 2). This suggests that apoE4- mut1 has much more exposed hydrophobic surfaces than apoE3. Both apoE3 and apoE4-mut1 are more stable than WT apoE4; however the difference in the midpoint of thermal denaturation $T_{1/2}$ between apoE3 and WT apoE4 is only ~2°C (40), in contrast to ~5°C difference between apoE4-mut1 and WT apoE4 (Table 1). This indicates significantly higher stability of apoE4-mut1 compared to apoE3.

Remarkably, we found earlier that two mutants of human apoA-I, the apoAI[E110A/E111A] and apoA-I[Δ(61–78)], that induce severe hypertriglyceridemia in mice had a more loosely folded structure and decreased stability compared to WT apoA-I, which does not induce hypertriglyceridemia (28,29). These structural changes in the apoA-I mutants facilitate their binding to TG-rich large lipoproteins (28,59). Thus, the association of a destabilized, loosely folded structure and the increased affinity to TGrich lipoproteins with hypertriglyceridemia is observed for both apoE4 and apoA-I. In this connection, it will be interesting to study other variant forms of the apolipoproteins that induce or correct hypertriglyceridemia.

In summary, our data show that the apoE4-mut1 variant that prevents the induction of hypertriglyceridemia has a more stable and compactly folded conformation, a decreased rate and ability to solubilize phospholipid vesicles, and a reduced ability to bind to large TG-rich particles. These properties of apoE4-mut1 may lead to enhanced lipolysis and receptor-mediated clearance of the apoE4-mut1-containing lipoprotein particles. The mutation apoE4-mut2 that results in milder hypertriglyceridemia leads to smaller or insignificant changes in the biophysical properties of apoE4. Overall, these data provide new biophysical insights into structure-function relationships of apoE4 that may underlie prevention of hypertriglyceridemia. The molecular etiology of common forms of hypertriglyceridemia in humans remains unknown. It is possible that structural mutations that destabilize apoE, apoA-I, or other apolipoproteins may contribute to hypertriglyceridemia in humans (60). Understanding the molecular mechanisms that underlie the improved biological properties of the apoE variant forms may facilitate the development of new therapeutic approaches for correction of lipid disorders in humans. For example, using small molecules that potentially can bind to apoE4 in vivo and modulate the protein biophysical properties (reviewed in ref. 61) may be one of the therapeutic strategies.

Abbreviations

ANS, 8-Anilino-2-naphthalene-sulfonate
apo, apolipoprotein
apoE$^{-/-}$, apoE-deficient
CD, circular dichroism
DMPC, dimyristoylphosphatidylcholine
GdnHCL, guanidine hydrochloride
LDL, low density lipoprotein(s)
LPL, lipoprotein lipase
PC, phosphatidylcholine
TG, triglyceride
VLDL, very low density lipoprotein(s)
WMF, wavelength of maximum fluorescence
WT, wild type

NIH-PA Author Manuscript

NIH-PA Author Manuscript

NIH-PA Author Manuscript

ACKNOWLEDGMENT

We thank Dr. Donald M. Small for helpful discussions and reading the manuscript prior to publication, Drs. Haya Herscovitz and Olga Gursky for advice, and Cheryl England and Michael Gigliotti for help with analytical procedures.

REFERENCES

1. Weisgraber KH. Apolipoprotein E: structure-function relationships. Adv. Protein Chem 1994;45:249–302. [PubMed: 8154371]
2. Mahley RW. Apolipoprotein E: cholesterol transport protein with expanding role in cell biology. Science 1988;240:622–630. [PubMed: 3283935]
3. Zannis, VI.; Kypreos, KE.; Chroni, A.; Kardassis, D.; Zanni, EE. Lipoproteins and atherogenesis. In: Loscalzo, J., editor. Molecular Mechanisms of Atherosclerosis. New York: Taylor & Francis; 2004. p. 111-174.
4. Zannis VI, Just PW, Breslow JL. Human apolipoprotein E isoprotein subclasses are genetically determined. Am.J. Hum. Genet 1981;33:11–24. [PubMed: 7468588]
5. Weisgraber KH, Rail SC Jr, Mahley RW. Human E apoprotein heterogeneity. Cysteine-arginine interchanges in the amino acid sequence of the apo-E isoforms. J Biol Chem 1981;256:9077–9083. [PubMed: 7263700]
6. Strittmatter WJ, Roses AD. Apolipoprotein E and Alzheimer disease. Proc. Natl. Acad. Sci. U. S. A 1995;92:4725–4727. [PubMed: 7761390]
7. Davidson J. Apolipoprotein E and atherosclerosis: beyond lipid effect. Arterioscler. Thromb. Vase. Biol 2005;25:267–269.
8. Havel RJ, Kotite L, Vigne JL, Kane JP, Tun P, Phillips N, Chen GC. Radioimmunoassay of human arginine-rich apolipoprotein, apoprotein E. Concentration in blood plasma and lipoproteins as affected by apoprotein E-3 deficiency. J. Clin. Invest 1980;66:1351–1362. [PubMed: 7440719]
9. Huang Y, Liu XQ, Rall SC, Taylor JM, von Eckardstein A, Assmann G, Mahley RW. Overexpression and accumulation of apolipoprotein E as a cause of hypertriglyceridemia. J. Biol. Chem 1998;273:26388–26393. [PubMed: 9756870]
10. Kypreos KE, Morani P, van Dijk KW, Havekes LM, Zannis VI. The amino-terminal 1–185 domain of apoE promotes the clearance of lipoprotein remnants in vivo. The carboxy-terminal domain is required for induction of hyperlipidemia in normal and apoE-deficient mice. Biochemistry 2001;22:6027–6035. [PubMed: 11352738]
11. Kypreos KE, van Dijk KW, van Der Zee A, Havekes LM, Zannis VI. Domains of apolipoprotein E contributing to triglyceride and cholesterol homeostasis in vivo. Carboxyl-terminal region 203–299 promotes hepatic very low density lipoprotein-triglyceride secretion. J. Biol. Chem 2001;276:19778–19786. [PubMed: 11279066]
12. Wilson C, Wardell MR, Weisgraber KH, Mahley RW, Agard DA. Three-dimensional structure of the LDL receptor-binding domain of human apolipoprotein E. Science 1991;252:1817–1822. [PubMed: 2063194]
13. Nolte RT, Atkinson D. Conformational analysis of apolipoprotein A-I and E-3 based on primary sequence and circular dichroism. Biophys. J 1992;63:1221–1239. [PubMed: 1477274]
14. Segrest JP, Jones MK, De Loof H, Brouillette CG, Venkatachalapathi YV, Anantharamaiah GM. The amphipathic helix in the exchangeable apolipoproteins: a review of secondary structure and function. J. Lipid Res 1992;33:141–166. [PubMed: 1569369]
15. Hatters DM, Peters-Libeu CA, Weisgraber KH. Apolipoprotein E structure: insights into function. Trends in Biochem. Sci 2006;31:445–454. [PubMed: 16820298]
16. Tanaka M, Vedhachalam C, Sakamoto T, Dhanasekaran P, Phillips MC, Lund-Katz S, Saito H. Effect of carboxyl-terminal truncation on structure and lipid interaction of human apolipoprotein E4. Biochemistry 2006;45:4240–4247. [PubMed: 16566598]
17. Kypreos KE, van Dijk KW, Havekes LM, Zannis VI. Generation of a recombinant apolipoprotein E variant with improved biological functions: hydrophobic residues (LEU-261, TRP-264, PHE-265, LEU-268, VAL-269) of apoE can account for the apoE-induced hypertriglyceridemia. J. Biol. Chem 2005;280:6276–6284. [PubMed: 15576362]

NIH-PA Author Manuscript

NIH-PA Author Manuscript

NIH-PA Author Manuscript

18. Westerlund JA, Weisgraber KH. Discrete carboxyl-terminal segments of apolipoprotein E mediate lipoprotein association and protein oligomerization. J. Biol. Chem 1993;268:15745–15750. [PubMed: 8340399]
19. Dong LM, Wilson C, Wardell MR, Simmons T, Mahley RW, Weisgraber KH, Agard DA. Human apolipoprotein E. Role of arginine 61 in mediating the lipoprotein preferences of the E3 and E4 isoforms. J. Biol. Chem 1994;269:22358–22365. [PubMed: 8071364]
20. Li X, Kypreos KE, Zanni EE, Zannis VI. Domains of apoE required for binding to apoE receptor 2 and to phospholipids: implications for the functions of apoE in the brain. Biochemistry 2003;42:10406–10417. [PubMed: 12950167]
21. Miller KW, Small DM. Triolein-cholesteryl oleate-cholesterol-lecithin emulsions: structural models of triglyceride-rich lipoproteins. Biochemistry 1983;22:443–451. [PubMed: 6824638]
22. Derksen A, Small DM. Interaction of ApoA-1 and ApoE-3 with triglyceride-phospholipid emulsions containing increasing cholesterol concentrations. Model of triglyceride-rich nascent and remnant lipoproteins. Biochemistry 1989;28:900–906. [PubMed: 2496752]
23. Dong LM, Weisgraber KH. Human apolipoprotein E4 domain interaction. Arginine 61 and glutamic acid 255 interact to direct the preference for very low density lipoproteins. J. Biol Chem 1996;271:19053–19057. [PubMed: 8702576]
24. Saito H, Dhanasekaran P, Baldwin F, Weisgraber KH, Phillips MC, Lund-Katz S. Effect of polymorphism on the lipid interaction of human apolipoprotein E. J. Biol. Chem 2003;278:40723–40729. [PubMed: 12917433]
25. Segall ML, Dhanasekaran P, Baldwin F, Anantharamaiah GM, Weisgraber KH, Phillips MC, Lund-Katz S. Influence of apoE domain structure and polymorphism on the kinetics of phospholipid vesicle solubilization. J Lipid Res 2002;43:1688–1700. [PubMed: 12364553]
26. Hatters DM, Peters-Libeu CA, Weisgraber KH. Engineering conformational destabilization into mouse apolipoprotein E. A model for a unique property of human apolipoprotein E4. J. Biol. Chem 2005;280:26477–26482. [PubMed: 15890642]
27. Gorshkova IN, Kypreos KE, Atkinson D, Zannis VI. Structure and stability of apolipoproteins A-I and E4 are altered by the mutations that affect plasma triglyceride concentration in mice, Protein. Science 2007;16:266.
28. Chroni A, Kan HY, Kypreos KE, Gorshkova IN, Shkodrani A, Zannis VI. Substitutions of glutamate 110 and 111 in the middle helix 4 of human apolipoprotein A-I (apoA-I) by alanine affect the structure and in vitro functions of apoA-I and induce severe hypertriglyceridemia in apoA-I-deficient mice. Biochemistry 2004;43:10442–10457. [PubMed: 15301543]
29. Gorshkova IN, Liu T, Kan HY, Chroni A, Zannis VI, Atkinson D. Structure and stability of apolipoprotein A-I in solution and in discoidal high-density lipoprotein probed by double charge ablation and deletion mutation. Biochemistry 2006;45:1242–1254. [PubMed: 16430220]
30. Li X, Kan HY, Lavrentiadou S, Krieger M, Zannis VI. Reconstituted discoidal apoE-phospholipid particles are ligands for the scavenger receptor BI. The amino-terminal 1–165 domain of apoE suffices for receptor binding. J. Biol. Chem 2002;277:21149–21157. [PubMed: 11861652]
31. Gorshkova IN, Liadaki K, Gursky O, Atkinson D, Zannis VI. Probing the lipid-free structure and stability of apolipoprotein A-I by mutation. Biochemistry 2000;39:15910–15919. [PubMed: 11123918]
32. Perugini MA, Schuck P, Howlett GJ. Self-association of human apolipoprotein E3 and E4 in the presence and absence of phospholipids. J. Biol. Chem 2000;275:36758–36765. [PubMed: 10970893]
33. Chen Y-H, Yang JT, Martinez HM. Determination of the secondary structures of proteins by circular dichroism and optical rotary dispersion. Biochemistry 1972;11:1420–1431.
34. John DM, Weeks KM. van't Hof enthalpies without baselines. Protein Science 2000;9:1416–1419. [PubMed: 10933511]
35. Pownall HJ, Massey JB, Kusserow SK, Gotto AM Jr. Kinetics of lipid--protein interactions: interaction of apolipoprotein A-I from human plasma high density lipoproteins with phosphatidylcholines. Biochemistry 1978;17:1183–1188. [PubMed: 207309]
36. Gorshkova IN, Liu T, Zannis VI, Atkinson D. Lipid-free structure and stability of apolipoprotein A-I: probing the central region by mutation. Biochemistry 2002;41:10529–10539. [PubMed: 12173940]

NIH-PA Author Manuscript

NIH-PA Author Manuscript

NIH-PA Author Manuscript

37. Satio H, Dhanasekaran P, Baldwin F, Weisgraber KH, Lund-Katz S, Phillips MC. Lipid binding-induced conformational change in human apolipoprotein E. Evidence for two lipid-bound states on spherical particles. J. Biol. Chem 2001;276:40949–40954. [PubMed: 11533033]
38. Lowry OH, Rosebrough NJ, Farr AL, Randall RJ. Protein measurement with the Folin phenol reagent. J. Biol. Chem 1951;193:265–275. [PubMed: 14907713]
39. Bartlett GR. Phosphorus assay in column chromatography. J. Biol. Chem 1959;234:466–468. [PubMed: 13641241]
40. Sakamoto T, Tanaka M, Vedhachalam C, Nickel M, Nguyen D, Dhanasekaran P, Phillips MC, Lund-Katz S, Saito H. Contributions of the carboxylterminal helical segment to the self-association and lipoprotein preferences of human apolipoprotein E3 and E4 isoforms. Biochemistry 2008;47:2968–2977. [PubMed: 18201068]
41. Acharya P, Segall ML, Zaiou M, Morrow J, Weisgraber KH, Phillips MC, Lund-Katz S, Snow J. Comparison of the stabilities and unfolding pathways of human apolipoprotein E isoforms by differential scanning calorimetry and circular dichroism. Biochim. Biophys. Acta 2002;1584:9–19. [PubMed: 12213488]
42. Morrow JA, Segall ML, Lund-Katz S, Phillips MC, Knapp M, Rupp B, Weisgraber KH. Differences in stability among the human apolipoprotein E isoforms determined by the amino-terminal domain. Biochemistry 2000;39:11657–11666. [PubMed: 10995233]
43. Satio H, Dhanasekaran P, Nguyen D, Holvoet P, Lund-Katz S, Phillips MC. Domain structure and lipid interaction in human apolipoprotein A-I and E, a general model. J. Biol. Chem 2003;278:23227–23232. [PubMed: 12709430]
44. Tall AR, Small DM, Deckelbaum RJ, Shipley GG. Structure and thermodynamic properties of high density lipoprotein recombinants. J Biol Chem 1977;252:4101–4111.
45. 1bdah JA, Phillips MC. Effects of lipid composition and packing on the adsorption of apolipoprotein A-I to lipid monolayers. Biochemistry 1988;27:7155–7162. [PubMed: 3143410]
46. Wang L, Atkinson D, Small DM. Interfacial properties of an amphipathic alpha-helix consensus peptide of exchangeable apolipoproteins at air/water and oil/water interfaces. J Biol Chem 2003;278:37480–37491. [PubMed: 12842901]
47. Nagle JF, Tristram-Nagle S. Lipid bilayer structure. Curr. Opin. Struc Biol 2000;10:474–480.
48. Rensen PC, van Berkel TJ. Apolipoprotein E effectively inhibits lipoprotein lipase-mediated lipolysis of chylomicron-like triglyceride-rich lipid emulsions in vitro and in vivo. J Biol. Chem 1996;271:14791–14799. [PubMed: 8662966]
49. Innerarity TL, Weisgraber KH, Arnold KS, Rail SC Jr, Mahley RW. Normalization of receptor binding of apolipoprotein E2. Evidence for modulation of the binding site conformation. J. Biol. Chem 1984;259:7261–7267. [PubMed: 6327714]
50. Hatters DM, Budamagunta MS, Voss JC, Weisgraber KH. Modulation of apolipoprotein E structure by domain interaction: differences in lipidbound and lipid-free forms. J. Biol. Chem 2005;280:34288–34295. [PubMed: 16076841]
51. Ma J, Yee A, Brewer HB Jr, Das S, Potter H. Amyloid-associated proteins alpha 1-antichymotrypsin and apolipoprotein E promote assembly of Alzheimer beta-protein into filaments. Nature 1994;372:45–46. [PubMed: 7969418]
52. Morrow JA, Hatters DM, Lu B, Hochtl P, Oberg KA, Rupp B, Weisgraber KH. Apolipoprotein E4 forms a molten globule. A potential basis for its association with disease. J.Biol. Chem 2002;277:50380–50385. [PubMed: 12393895]
53. Segrest JP, Garber DW, Brouillettee CG, Harvey SC, Anantharamaian GM. The amphipathic alpha helix: a multifunctional structural motif in plasma apolipoproteins. Adv. Protein Chem 1994;45:303–369. [PubMed: 8154372]
54. Huang Y, Liu XQ, Rail SC Jr, Mahley RW. Apolipoprotein E2 reduces the low density lipoprotein level in transgenic mice by impairing lipoprotein lipase-mediated lipolysis of triglyceride-rich lipoproteins. J. Biol. Chem 1998;273:17483–17490. [PubMed: 9651338]
55. Hospattankar AV, Fairwell T, Ronan R, Brewer HB Jr. Amino acid sequence of human plasma apolipoprotein C-II from normal and hyperlipoproteinemic subjects. J. Biol Chem 1984;259:318–322. [PubMed: 6706938]

NIH-PA Author Manuscript

NIH-PA Author Manuscript

NIH-PA Author Manuscript

56. Drury J, Narayanaswami V. Examination of lipid-bound conformation of apolipoprotein E4 by pyrene excimer fluorescence. J. Biol. Chem 2005;280:14605–14610. [PubMed: 15708851]

57. Narayanaswami V, Ryan RO. Molecular basis of exchangeable apolipoprotein function. Biochem. Biophys. Acta 2000;1483:15–36. [PubMed: 10601693]

58. Saito H, Lund-Katz S, Phillips MC. Contributions of domain structure and lipid interaction to the functionality of exchangeable human apolipoproteins. Prog. Lipid Res 2004;43:350–380. [PubMed: 15234552]

59. Chroni A, Kan HY, Shkodrani A, Liu T, Zannis VI. Deletions of helices 2 and 3 of human apoA-I are associated with severe dyslipidemia following adenovirus-mediated gene transfer in apoA-I-deficient mice. Biochemistry 2005;44:4108–4117. [PubMed: 15751988]

60. Mahley, RW.; Rail, SC, Jr.. Type III hyperlipoproteinemia (dysbetalipoproteinemia): The role of apolipoprotein E in normal and abnormal lipoprotein metabolism. In The Metabolic & Molecular Bases of Inherited Disease. In: Scriver, CR.; Beaudet, AL.; Valle, D.; Sly, WS., editors. New York: McGraw-Hill; 2001. p. 2835-2862.

61. Mahley RW, Weisgraber KH, Huang Y. Apolipoprotein E4: a causative factor and therapeutic target in neuropathology, including Alzheimer's disease. Proc. Natl. Acad. Sci. U. S A 2006;103:5644–5651. [PubMed: 16567625]

NIH-PA Author Manuscript
NIH-PA Author Manuscript
NIH-PA Author Manuscript

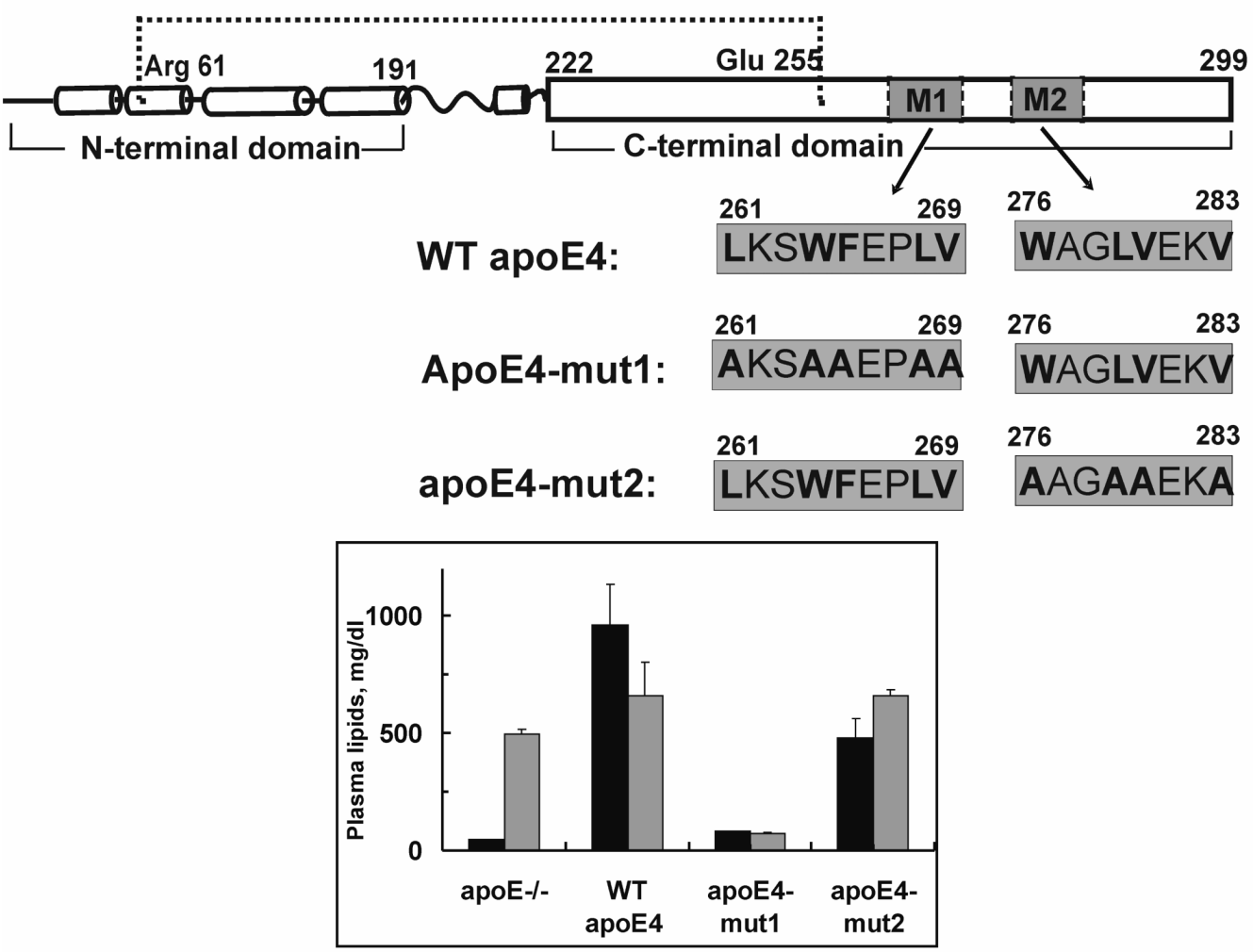

Figure 1.

Mutations introduced in apoE4-mut1 and apoE4-mut2. In the schematic representation of apoE4 (the top), cylinders represent helical structures in the N-terminal domain (amino acids 1–191) based on the X-ray crystallography structure of the isolated domain (12). The rectangle and the wavy line represent the C-terminal domain (amino acids 222–299) and linker, respectively. Their structures are unknown; the C-terminal domain is thought to be mostly helical and the linker is disordered, on the basis of structural prediction and CD spectroscopy (13–16). The shaded areas M1 and M2 show sites of the mutations introduced in apoE4-mut1 and apoE4-mut2, respectively. The shaded blocks below the schematic representation of apoE4 show the amino acid sequences of the corresponding segments (amino acids 261–269 and 276–283) for WT apoE4, apoE4-mut1, and apoE4-mut2; the mutated residues are shown in bold. The dotted line indicates a putative salt bridge between Arg61 and Glu255 that stabilizes a closer contact between the N- and C-terminal domains in the tertiary structure. Inset: Effects of high level expression of the apoE4 variants on plasma lipid levels in apoE$^{-/-}$mice. Plasma TG (black columns) and cholesterol (gray columns) concentrations in apoE$^{-/-}$ mice are shown before (apoE$^{-/-}$) and four days after infection with recombinant adenoviruses expressing WT apoE4, apoE4-mut1, or apoE4-mut2. Adopted from ref. 17.

NIH-PA Author Manuscript

NIH-PA Author Manuscript

NIH-PA Author Manuscript

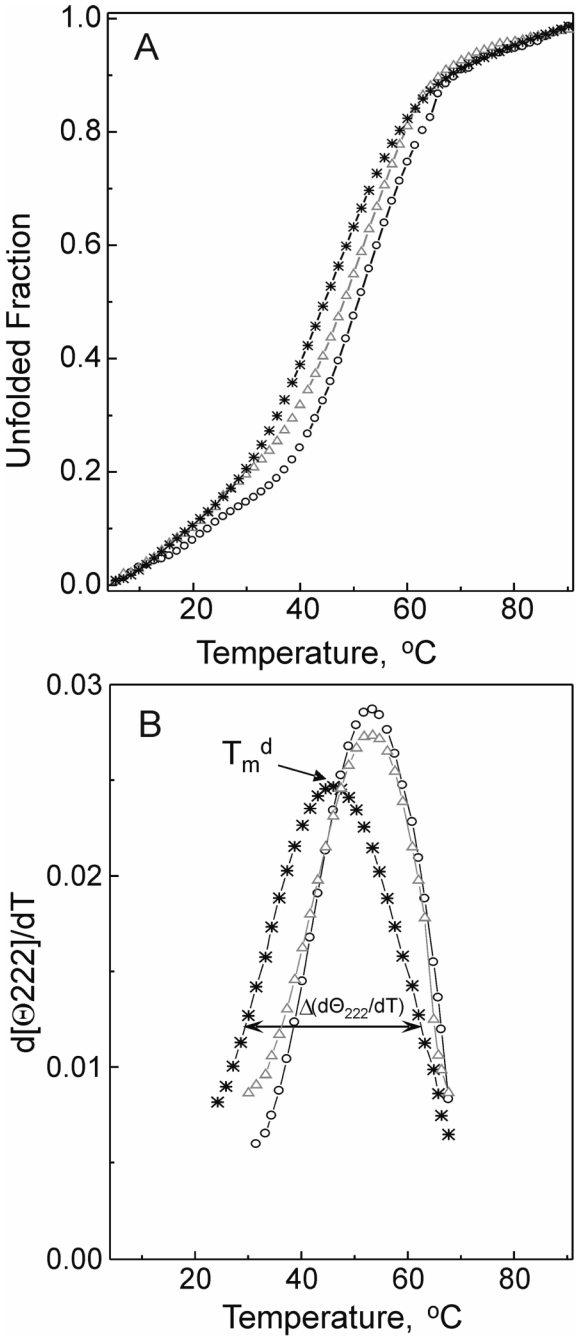

Figure 2.

Thermal unfolding of the apoE4 variants. (A) Thermal unfolding curves for the apoE4 forms are derived from a fractional change in CD ellipticity at wavelength of 222 nm, (Θ_{222}), at increasing temperature. Protein concentration was 15 μg/mL. (B) First derivative functions $d(\Theta_{222})/dT$ of the thermal unfolding curves. The derivative curves are shown in the temperature region ~27 to ~70°C that corresponds to more cooperative structural changes. The peak position that determines the apparent melting temperature, T^d_m, and the width of the first derivative curve at the half of it maximal height, $\Delta(d\Theta_{222}/dT)$, are indicated for WT apoE4. WT apoE4 (black stars), apoE4-mut1 (open black circles), and apoE4-mut2 (open gray triangles).

NIH-PA Author Manuscript
NIH-PA Author Manuscript
NIH-PA Author Manuscript

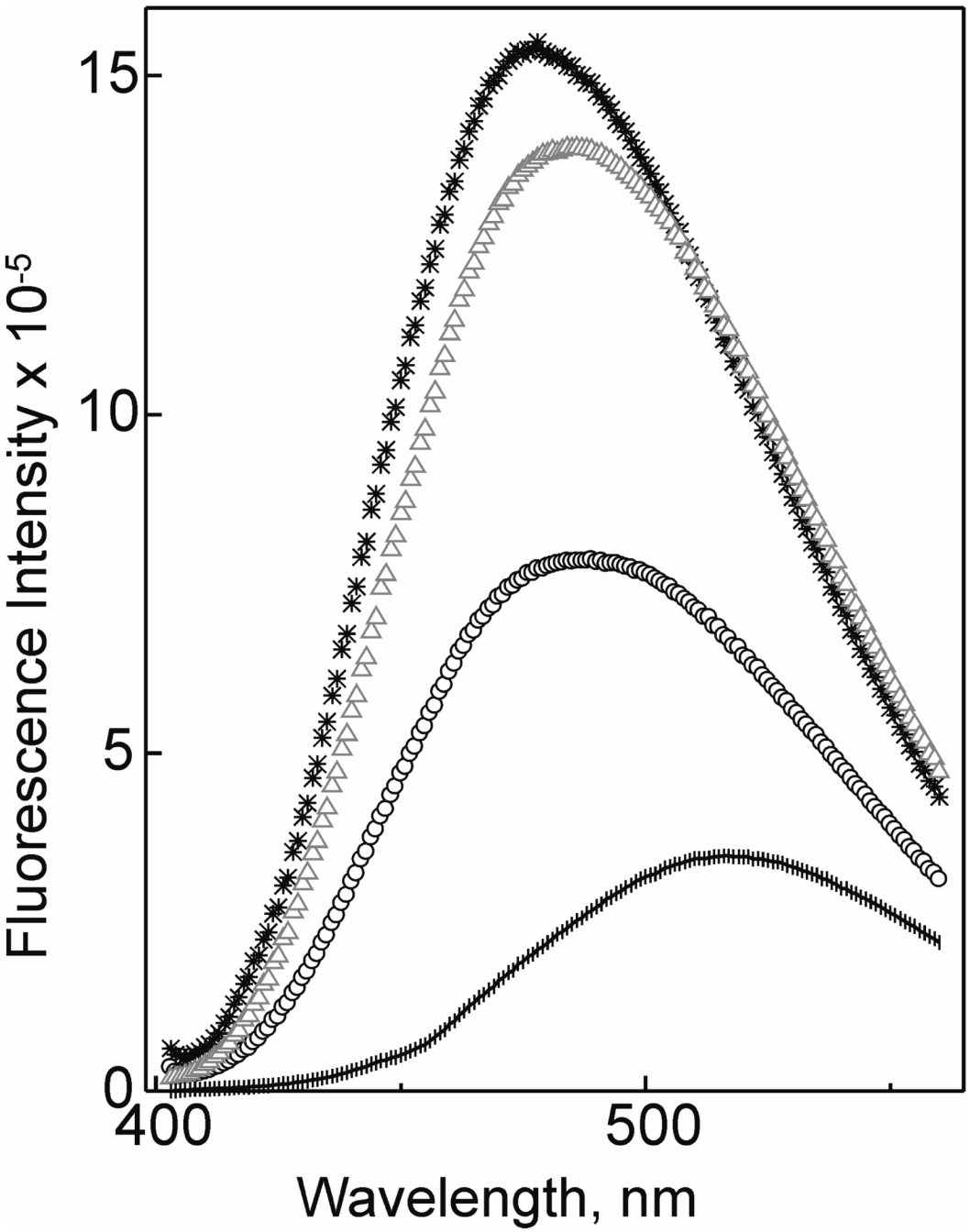

Figure 3.
ANS fluorescence recorded in the presence of the apoE4 variants. Fluorescence of ANS (125 μM) was recorded in the presence of 25 μg/ml WT apoE4 (black stars), apoE4-mut1 (open black circles), apoE4-mut2 (open gray triangles), carbonic anhydrase (bars), or in buffer alone (solid line). Two latter spectra are superimposed.

NIH-PA Author Manuscript
NIH-PA Author Manuscript
NIH-PA Author Manuscript

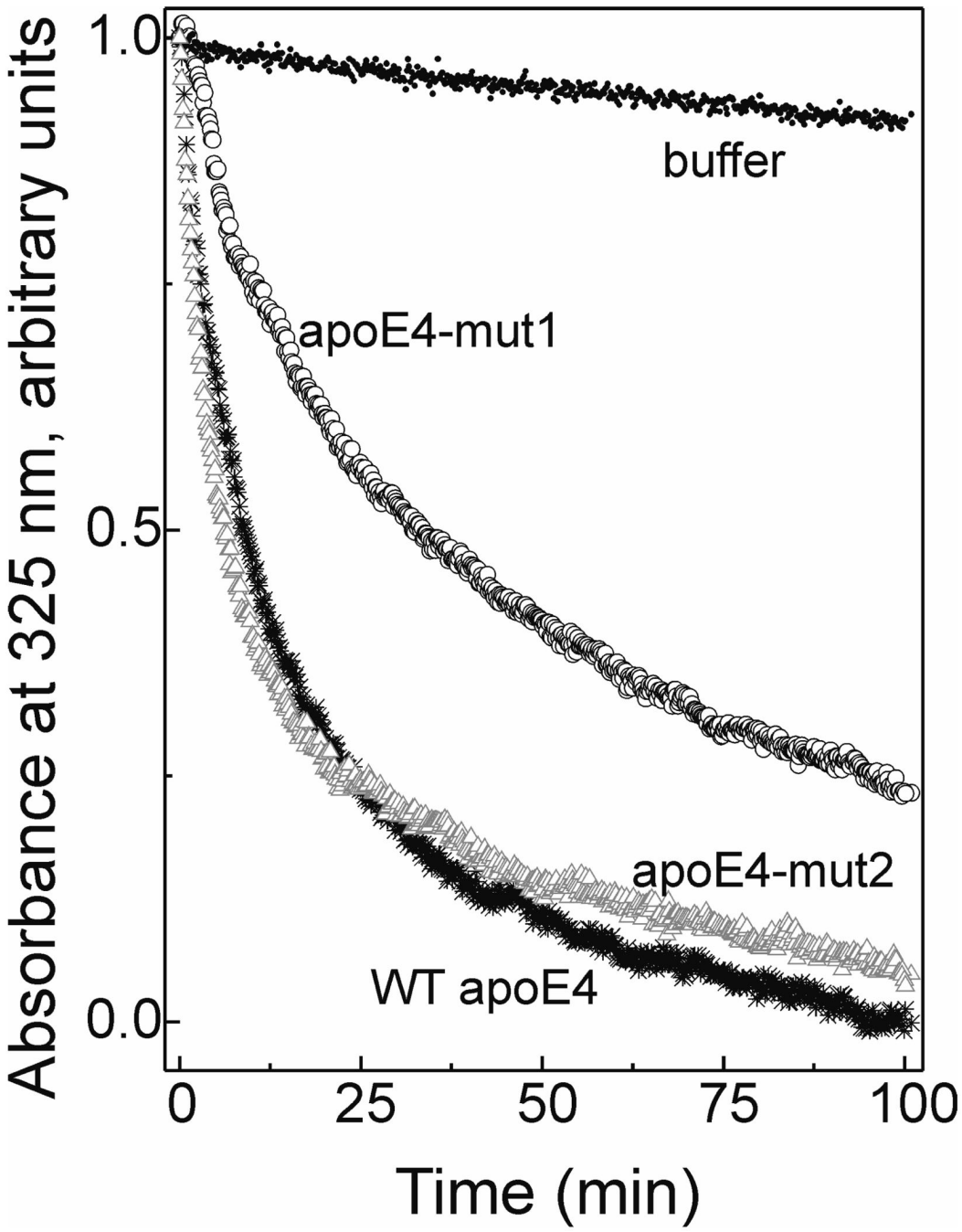

Figure 4.

The time course of DMPC turbidity clearance by the apoE variants. A small amount of protein or buffer was added to DMPC multilamellar vesicles (60 μg/ml) preincubated at 24°C to get the final protein concentration 7.5 μg/ml. The turbidity clearance was monitored by absorbance at 325 nm at the controlled temperature 24°C. WT apoE4 (black stars), apoE4-mut1 (open black circles), apoE4-mut2 (open gray triangles), and buffer alone (black dots).

NIH-PA Author Manuscript
NIH-PA Author Manuscript
NIH-PA Author Manuscript

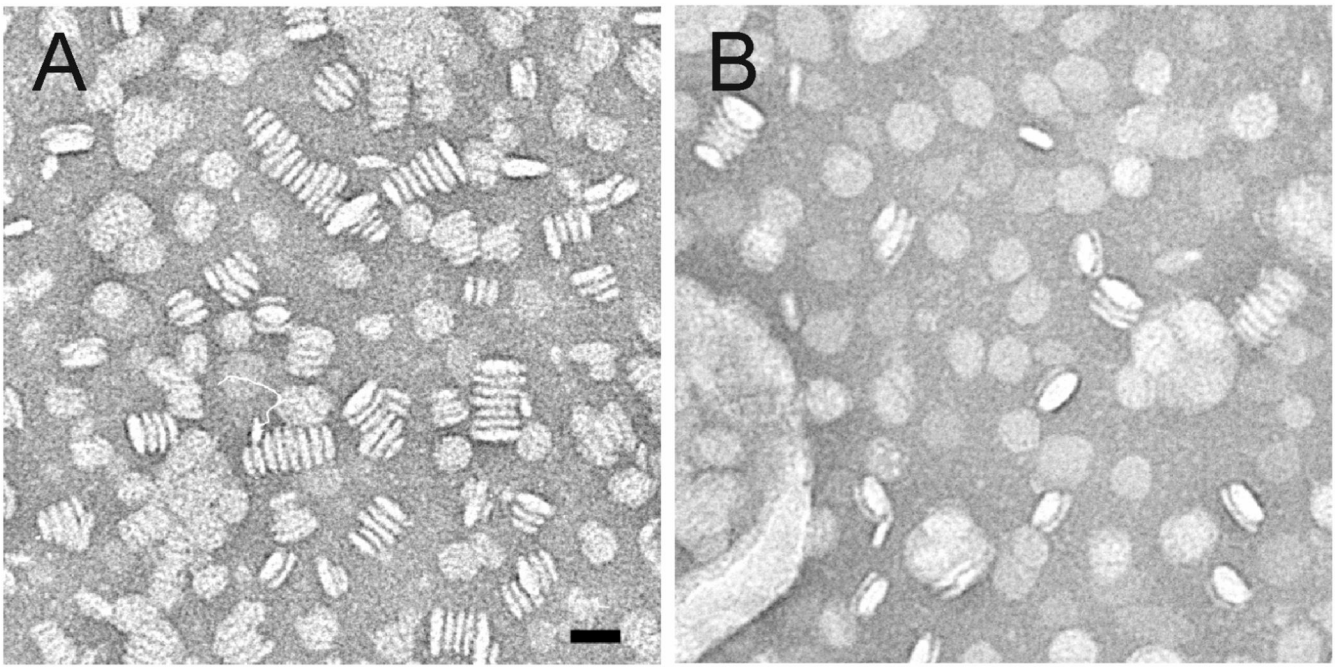

Figure 5.
Electron micrographs of negatively stained apoE4/DMPC mixtures. Mixtures of apoE4 (7.5 μg/ml) and DMPC multilamellar vesicles (60 μg/ml) were incubated for 20 h at 24°C before imaging by electron microscopy. The representative fields are shown for WT apoE4/DMPC (A) and apoE4-mut1/DMPC (B). The scale bar corresponds to 25 nm.

NIH-PA Author Manuscript
NIH-PA Author Manuscript
NIH-PA Author Manuscript

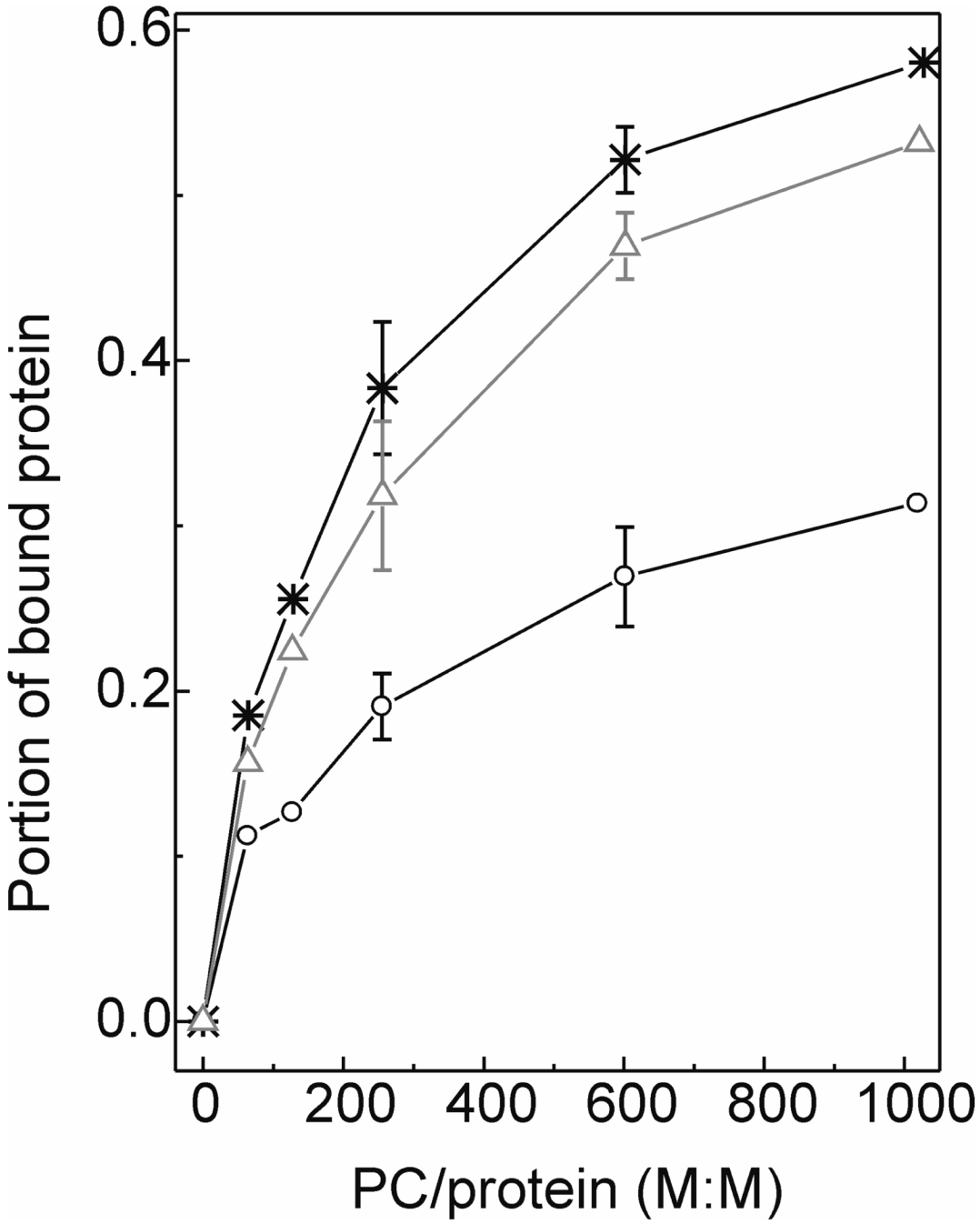

Figure 6.

Binding of the apoE4 variants to emulsion particles. Emulsion/apoE4 mixtures were incubated for 1 hr and then spun to separate bound and unbound protein. A portion of bound apoE4 was determined for various PC to protein molar ratios in the incubation mixtures. WT apoE4 (black stars), apoE4-mut1 (open black circles), or apoE4-mut2 (open gray triangles).

NIH-PA Author Manuscript
NIH-PA Author Manuscript
NIH-PA Author Manuscript

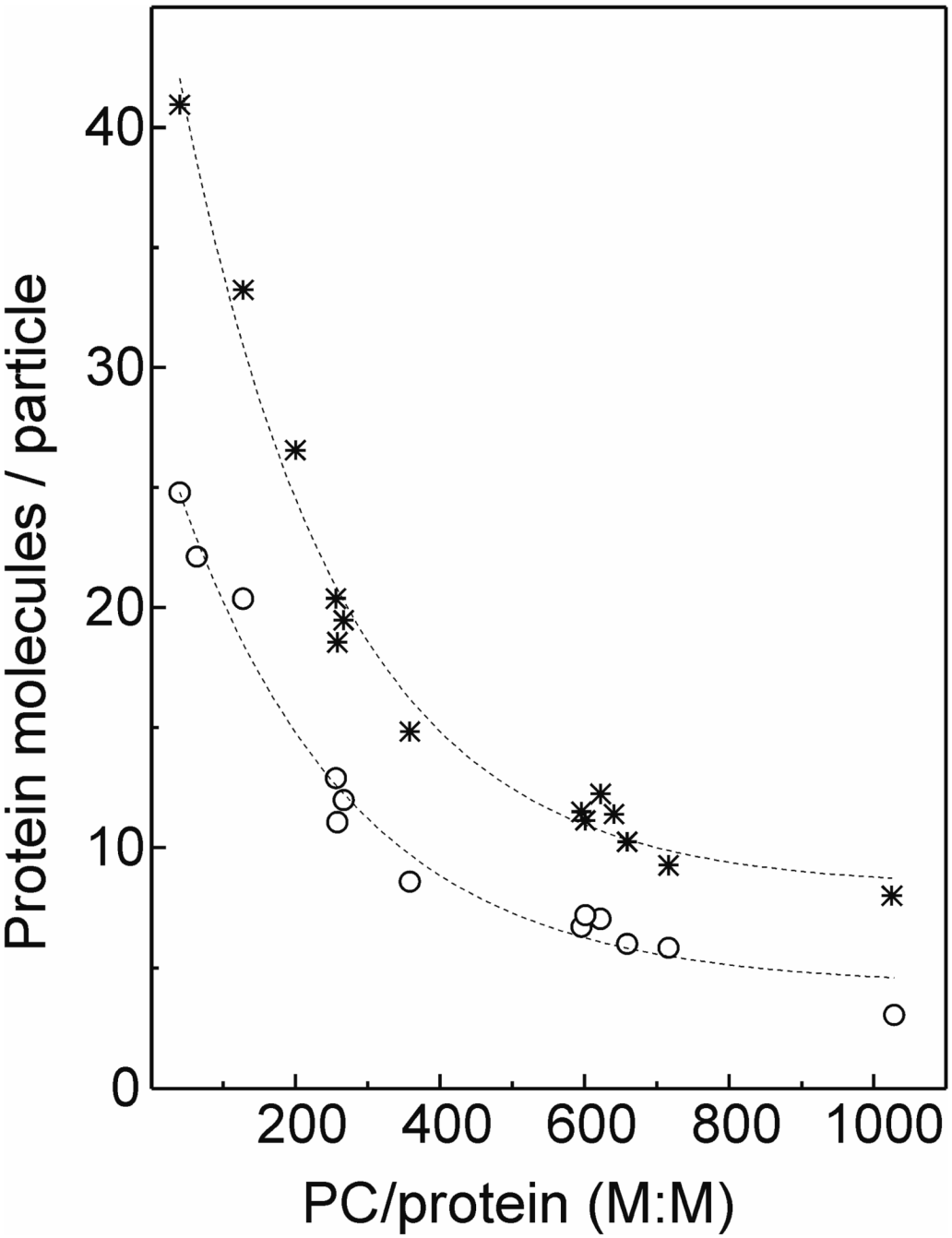

Figure 7.
Bound apoE4 molecules per emulsion particle. Numbers of the bound protein molecules per particle were estimated at various PC to protein molar ratios in the incubation mixtures. See "Results" for details. WT apoE4 (stars), apoE4-mut1 (open circles).

NIH-PA Author Manuscript NIH-PA Author Manuscript NIH-PA Author Manuscript

Table 1

α-helical Content and Parameters of Thermal Denaturation for WT and the Variant Forms of apoE4 Determined by Far-UV CD[a]

apoE4	α-helix[b] (%)	Number of residues in α-helix [c]	$T_{1/2}$ [d] °C	T_m [d], °C	Δ($d[\Theta_{222}]/dT$)[d], °C
WT apoE4	62 ± 3	~189	46 ± 0.5	47 ± 0.5	33 ± 1.0
apoE4-mut2	60 ± 2	~183 (−6)	49 ± 1.3 [e]	52 ± 1.3 [f]	27 ± 1.5 [f]
apoE4-mut1	51 ± 2[f,h]	~155 (−34)	51 ± 0.5 [g]	53 ± 1 [g]	25 ± 0.6 [g]

[a] Values are means ± SD from three to five experiments.

[b] Estimated from the value $[\Theta_{222}]$ at 25 °C according to ref. 33 ; systematic error is ±3%, statistical error is within ±2%.

[c] Values in parenthesis show changes in the number of residues compared to WT apoE4.

[d] Parameters determined from the thermal unfolding curves; systematic error is within ±1°C. $T_{1/2}$ is the midpoint of thermal unfolding. T_m is a maximum of the first derivative function $d[\Theta_{222}]/dT$; Δ($d[\Theta_{222}]/dT$) is the width of the first derivative function $d[\Theta_{222}]/dT$ at the half maximal height.

[e] Significance of differences from the value for WT apoE4: $p<0.05$.

[f] Significance of differences from the value for WT apoE4: $p<0.01$.

[g] Significance of differences from the value for WT apoE4: $p<0.005$.

[h] Significance of differences from the value for apoE4-mut2: $p<0.01$.

NIH-PA Author Manuscript

NIH-PA Author Manuscript

NIH-PA Author Manuscript

Table 2

ANS Fluorescence in the Presence of WT and the Variant Forms of apoE4 and Reference Proteins.

protein	*I* (relative units)	WMF (nm)
apoE WT	1.0	478
apoE-mut1	0.5	487
apoE-mut2	0.9	484
Bovine serum albumin	2.9	475
Carbonic anhydrase	0.2	516
ANS in buffer alone	0.2	516

Fluorescence of ANS (125 μM) was recorded in the presence of 0.025 mg/ml apoE4 WT, apoE4-mut1, apoE4-mut2, carbonic anhydrase, or bovine serum albumin or in Tris buffer alone. *I* is ANS fluorescence intensity in relative units compared to the fluorescence in Tris buffer alone.

NIH-PA Author Manuscript

NIH-PA Author Manuscript

NIH-PA Author Manuscript

Table 3

Binding of WT and the Variant Forms of apoE4 to TG-Rich Emulsion Particles[a].

apoE4	PC to protein molar ratio in the incubation mixtures			
	255 ± 5		600 ± 7	
	Portion of the bound protein [b]	Protein on the emulsion particles [c] (amino acids/mol PC)	Portion of the bound protein [b]	Protein on the emulsion particles [c] (amino acids/mol PC)
WT apoE4	0.39 ± 0.04	0.71 ± 0.08	0.53 ± 0.02	0.41 ± 0.03
apoE4-mut2	0.32 ± 0.04	0.59 ± 0.10	0.47 ± 0.02	0.37 ± 0.07
apoE4-mut1	0.19 ± 0.02 [d, g]	0.38 ± 0.007 [e, h]	0.28 ± 0.03 [d, f]	0.23 ± 0.02 [d, g]

[a] Values are means ± SD from three to five experiments.

[b] Portion of the bound protein of the total protein added to emulsion.

[c] Parameter derived from composition of apoE4-emulsion complexes recovered by ultracentrifugation following the incubation of apoE4 with emulsion.

[d] Significance of difference from the value for WT apoE4: $p<0.005$.

[e] Significance of difference from the value for WT apoE4: $p<0.01$.

[f] Significance of difference from the value for apoE4-mut2: $p<0.005$.

[g] Significance of difference from the value for apoE4-mut2: $p<0.05$.

[h] Significance of difference from the value for apoE4-mut2: $0.1<p<0.05$.